Supporting Information

Structure-dependent mercury sequestration and microbial methylation mediated by FeS nanoparticles in contaminated groundwater

Xiaoyu Huang[a], Luyao Sun[a], Xianjin Tang[b], Yanyan Gong*[a]

[a] *College of Environment and Climate, Guangdong Provincial Key Laboratory of Environmental Pollution and Health, Jinan University, Guangzhou 511443, China*

[b] *Zhejiang Provincial Key Laboratory of Agricultural Resources and Environment, College of Environmental and Resource Sciences, Zhejiang University, Hangzhou 310058, China*

*Corresponding author. E-mail address: yanyangong@jnu.edu.cn (Y. Gong).

This supporting information includes 20 pages, 3 tables, and 9 figures.

Contents

Figure S7. Linear relationship between S^{2-} to Hg^{2+} molar ratios and Hg(II) removal efficiency

Figure S8. Dynamics of net mercury methylation by G. *sulfurreducens* PCA cultures exposed to Hg(II) before and after sorption, coprecipitation, and chemical precipitation with CMC-FeS at various S^{2-} to Hg^{2+} molar ratios

Figure S9. Optical density (OD_{600}) of *G. sulfurreducens* PCA cultures exposed to Hg(II) after sorption, coprecipitation, and chemical precipitation with CMC-FeS

Section S1. Materials

All reagents used in this study were of analytical grade or higher. Iron Sulfate heptahydrate ($FeSO_4 \cdot 7H_2O$), sodium sulfide nonahydrate ($Na_2S \cdot 9H_2O$), CMC (sodium salt, MW = 90000, degree of substitute = 0.7), mercury nitrate ($Hg(NO_3)_2$), sodium sulfate (Na_2SO_4), potassium phosphate dibasic solution (K_2HPO_4), and potassium phosphate monobasic (KH_2PO_4) were purchased from Jiangyang Global Reagent Technology (Taizhou, China). Sodium bicarbonate ($NaHCO_3$) was obtained from Damao Chemical Reagent Technology (Tianjin, China). Calcium chloride anhydrous ($CaCl_2$) and sodium chloride (NaCl) were acquired from Guangzhou Chemical Reagent Technology (Guangzhou, China). Ascorbic acid, fumaric acid, magnesium sulfate hexahydrate ($MgSO_4 \cdot 7H_2O$), $NaActate \cdot 3H_2O$, resazurin biotin, pantothenic acid, p-aminobenzoic acid, nicotinic acid, thiamine, riboflavin, pyridoxine HCl, and folic acid were obtained from Aladdin industrial corporation (Shanghai, China). Glacial acetic acid, sodium acetate, and cysteine were obtained from Sinopharm Chemical Reagent Corporation (Shanghai, China). Hg^{2+} stock solution (1000 mg L^{-1}) was prepared by dissolving $Hg(NO_3)_2$ in 28 mM HNO_3 solution.

Section S2. Preparation of CMC-FeS nanoparticles

CMC-FeS nanoparticles were synthesized according to a previously reported approach by Gong et al.[1] In brief, a CMC solution was first prepared with deionized (DI) water. Then, a solution of $FeSO_4$ was added to the CMC solution under N_2 purging to form Fe^{2+}-CMC complexes. Subsequently, a stoichiometric amount of Na_2S solution was introduced into the solution drop-wise under shaking and N_2 purging. The resultant nanoparticle suspension contained 100 mg L^{-1} FeS and 0.004% CMC. To ensure complete reaction and full growth of the nanoparticles, the suspension was sealed and aged for 24 h before use.

Section S3. Hg speciation analysis, cell density, and viability of the PCA cells

At predetermined time intervals (10, 24, 96 h), a set of four vials were sampled for Hg species distributions on the cell and in the solution. First, all samples were immediately analyzed for purgeable element Hg(0) by purging dissolved gaseous Hg(0) from the mixture. Secondly, two purged samples were filtered through 0.22 μm syringe filters (Jinteng Experimental Equipment Co., Ltd., Tian Jin, China) to remove cells, and the filtrate was analyzed for nonpurgeable soluble Hg (Hg_{sol}) and soluble MeHg ($MeHg_{sol}$). An aliquot from the other two purged samples was analyzed for total nonpurgeable Hg (Hg_{NP}) and total MeHg ($MeHg_{total}$). MeHg ($MeHg_{total}$ and $MeHg_{sol}$) samples were preserved in HCl (0.4% v/v) at 4°C until analysis. Hg samples (Hg_{NP} and Hg_{sol}) samples were preserved in BrCl (5% v/v) at 4°C until analysis. Total Hg (Hg_T) was calculated by the sum of Hg(0) and Hg_{NP}. The cell-associated nonpurgeable Hg (Hg_{cell}) was determined by subtracting Hg_{sol} from Hg_{NP}, and similarly for the cell-associated MeHg ($MeHg_{cell} = MeHg_{Total} - MeHg_{sol}$). The soluble and cell-associated inorganic Hg (IHg_{sol} or IHg_{cell}) were calculated by the difference between nonpurgeable Hg and MeHg (i.e., $IHg_{sol} = Hg_{sol} - MeHg_{sol}$ and $IHg_{cell} = Hg_{cell} - MeHg_{cell}$). The cell density was monitored by measuring the optical density (OD_{600}) with a Microplate reader (Epoch2, BioTek, Winooski, VT, U.S.A.). The viability of the cells was determined via a confocal laser scanning microscopy (CLSM) (LSM800, Zeiss, Jena, Germany) and the ratio of cell viability/total cell number was calculated using software Image-Pro Plus 6.0.

Section S4. Simulation of Hg methylation rate constant and MeHg demethylation rate constant

Eq. S1 describes the general kinetics for the Hg(II)-MeHg methylation-demethylation system, assuming pseudo first-order reactions for mercury methylation (described by the methylation rate constant, k_m) and demethylation (described by the demethylation rate constant, k_d):

$$\frac{d}{dt}\begin{bmatrix}[Hg(II)(t)]\\ [MeHg](t)\end{bmatrix} = \begin{bmatrix}-k_m & k_d\\ k_m & -k_d\end{bmatrix}\begin{bmatrix}[Hg(II)(t)]\\ [MeHg](t)\end{bmatrix} \quad \text{(S1)}$$

In this study, we solved **Eq. S1** and obtained the time-dependent concentration of MeHg (**Eq. S2**), which considered both demethylation and changes in MeHg and Hg(II) concentrations during the incubation.

$$[MeHg](t) = \left(\frac{k_d}{k_m + k_d}e^{-(k_m + k_d)t} + \frac{k_m}{k_m + k_d}\right)[MeHg]_{t=0} + \left(\frac{k_d}{k_m + k_d}\left(1 - e^{-(k_m + k_d)t}\right)\right)[Hg(II)]_{t=0} \quad \text{(S2)}$$

where *[MeHg](t)* is the concentration of MeHg (nM) at incubation time t (h), k_m represents methylation rate potential (h^{-1}), k_d represents demethylation rate constant (h^{-1}), $[MeHg]_{t=0}$ is initial MeHg concentration (nM), and $[Hg(II)]_{t=0}$ is initial concentration of inorganic Hg(II) (nM). In our study, $[MeHg]_{t=0}$ was 0 and $[Hg(II)]_{t=0}$ was 2991 nM. Therefore, **Eq. S2** was simplified to:

$$[MeHg](t) = 2991\frac{k_m}{k_m + k_d}\left(1 - e^{-(k_m + k_d)t}\right) \quad \text{(S3)}$$

The fitting of *[MeHg](t)* vs. t was conducted using SigmaPlot 12.5 software.

Table S1. Chemical compositions of the NBAF medium.[2, 3]

	Ingredient	Content in 1 L
100X NB Salts	KH_2PO_4	42 g
	K_2HPO_4	22 g
	NH_4Cl	20 g
	KCl	38 g
	NaCl	36 g
NB Mineral Elixir	Nitrilotriacetic acid	2.14 g
	$MnCl_2 \cdot 4H_2O$	0.1 g
	$FeSO_4 \cdot 7H_2O$	0.3 g
	$CoCl_2 \cdot 6H_2O$	0.17 g
	$ZnSO_4 \cdot 7H_2O$	0.2 g
	$CuCl_2 \cdot 2H_2O$	0.03 g
	$AlK(SO_4)_2 \cdot 12H_2O$	0.005 g
	H_3BO_3	0.005 g
	$Na_2MoO_4 \cdot 2H_2O$	0.09 g
	$NiSO_4 \cdot 6H_2O$	0.11 g
	$Na_2WO_4 \cdot 2H_2O$	0.02 g
DL Vitamins	Biotin	0.002 g
	Pantothenic Acid	0.005 g
	B-12	0.0001 g
	p-aminobenzoic acid	0.005 g
	Thioctic Acid	0.005 g
	Nicotinic Acid	0.005 g
	Thiamine	0.005 g
	Riboflavin	0.005 g
	Pyridoxine HCl	0.01 g
	Folic Acid	0.002 g
Medium compositions	Fumarate	4.64 g
	100X NB Salts	10 mL
	NB Mineral Elixir	10 mL
	DL vitamins	15 mL
	$CaCl_2 \cdot 2H_2O$	0.04 g L^{-1}
	$MgSO_4 \cdot 7H_2O$	0.10 g
	$NaHCO_3$	1.80 g
	Na_2CO_3	0.43 g
	1 mM Na_2SeO_4	1.0 mL
	Na Acetate$\cdot H_2O$	2.04 g
	Final pH adjusted to 7.0	

Table S2. Hyperfine parameters of Mössbauer spectra of Hg-CMC-FeS_{sorp} and Hg-CMC-FeS_{cpt}.

Sample	Isomer shift (mm s^{-1})	Quadrupole splitting (mm s^{-1})	Full width at half maximum (mm s^{-1})	Area (%)
Hg-CMC-FeS_{sorp}	0.34	0.73	0.23	100
Hg-CMC-FeS_{cpt}	0.35	0.75	0.23	100

Table S3. Simulated methylation rate constant k_m and demethylation rate k_d using a nonlinear reversible reaction model

Sample		Methylation rate constant, k_m (h^{-1})	SD	Demethylation rate constant, k_d (h^{-1})	SD	R^2
Various Hg forms	Hg(II)	2.23×10^{-3}	1.08×10^{-5}	1.01×10^{-1}	1.49×10^{-2}	0.987
	Hg(II) after sorption with CMC-FeS	1.12×10^{-3}	9.17×10^{-6}	7.28×10^{-2}	1.30×10^{-2}	0.970
	Hg(II) after coprecipitation with CMC-FeS	1.49×10^{-3}	3.85×10^{-6}	8.92×10^{-2}	8.99×10^{-3}	0.989
	Hg(II) after chemical precipitation with CMC-FeS	1.76×10^{-3}	8.26×10^{-6}	8.99×10^{-2}	1.39×10^{-2}	0.983
Particulate Hg phase	Hg-CMC-FeS_{sorp}	2.39×10^{-4}	4.07×10^{-7}	5.17×10^{-2}	4.00×10^{-3}	0.996
	Hg-CMC-FeS_{cpt}	4.08×10^{-4}	2.02×10^{-6}	6.15×10^{-2}	7.99×10^{-3}	0.985
	Hg-CMC-FeS_{pre}	2.77×10^{-4}	2.24×10^{-6}	6.47×10^{-2}	1.09×10^{-2}	0.976
Hg(II) after sorption with CMC-FeS at various $S^{2-}$to Hg^{2+} molar ratios	0.068:1	1.51×10^{-3}	3.54×10^{-6}	8.54×10^{-2}	6.99×10^{-3}	0.966
	0.23:1	1.34×10^{-3}	3.71×10^{-6}	8.06×10^{-2}	6.70×10^{-3}	0.979
	0.57:1	1.12×10^{-3}	1.05×10^{-5}	7.28×10^{-2}	1.39×10^{-2}	0.909
Hg(II) after coprecipitation with CMC-FeS at various $S^{2-}$to Hg^{2+} molar ratios	0.068:1	1.98×10^{-3}	1.16×10^{-6}	1.00×10^{-1}	1.39×10^{-2}	0.972
	0.23:1	1.75×10^{-3}	1.15×10^{-5}	9.62×10^{-2}	1.49×10^{-2}	0.971
	0.57:1	1.52×10^{-3}	8.27×10^{-6}	9.14×10^{-2}	1.39×10^{-2}	0.937
Hg(II) after chemical precipitation with CMC-FeS at various $S^{2-}$to Hg^{2+} molar ratios	0.068:1	2.28×10^{-3}	3.67×10^{-6}	1.03×10^{-1}	6.99×10^{-3}	0.992
	0.23:1	2.02×10^{-3}	1.32×10^{-6}	9.59×10^{-2}	3.99×10^{-3}	0.997
	0.57:1	1.78×10^{-3}	7.77×10^{-6}	8.82×10^{-2}	9.99×10^{-3}	0.980

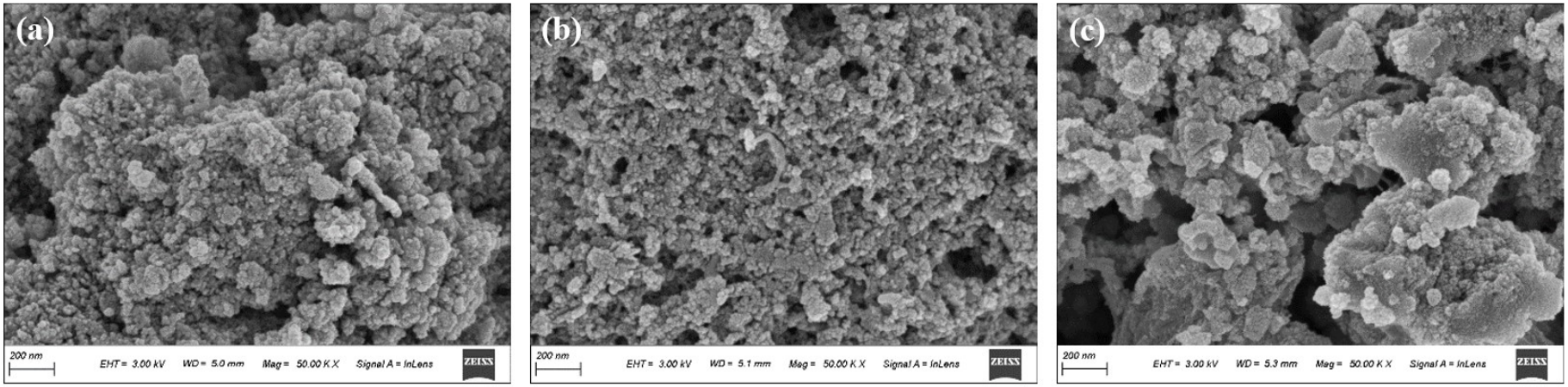

Figure S1. SEM images of (a) Hg-CMC-FeS_{sorp}, (b) Hg-CMC-FeS_{cpt}, and (c) Hg-CMC-FeS_{pre}.

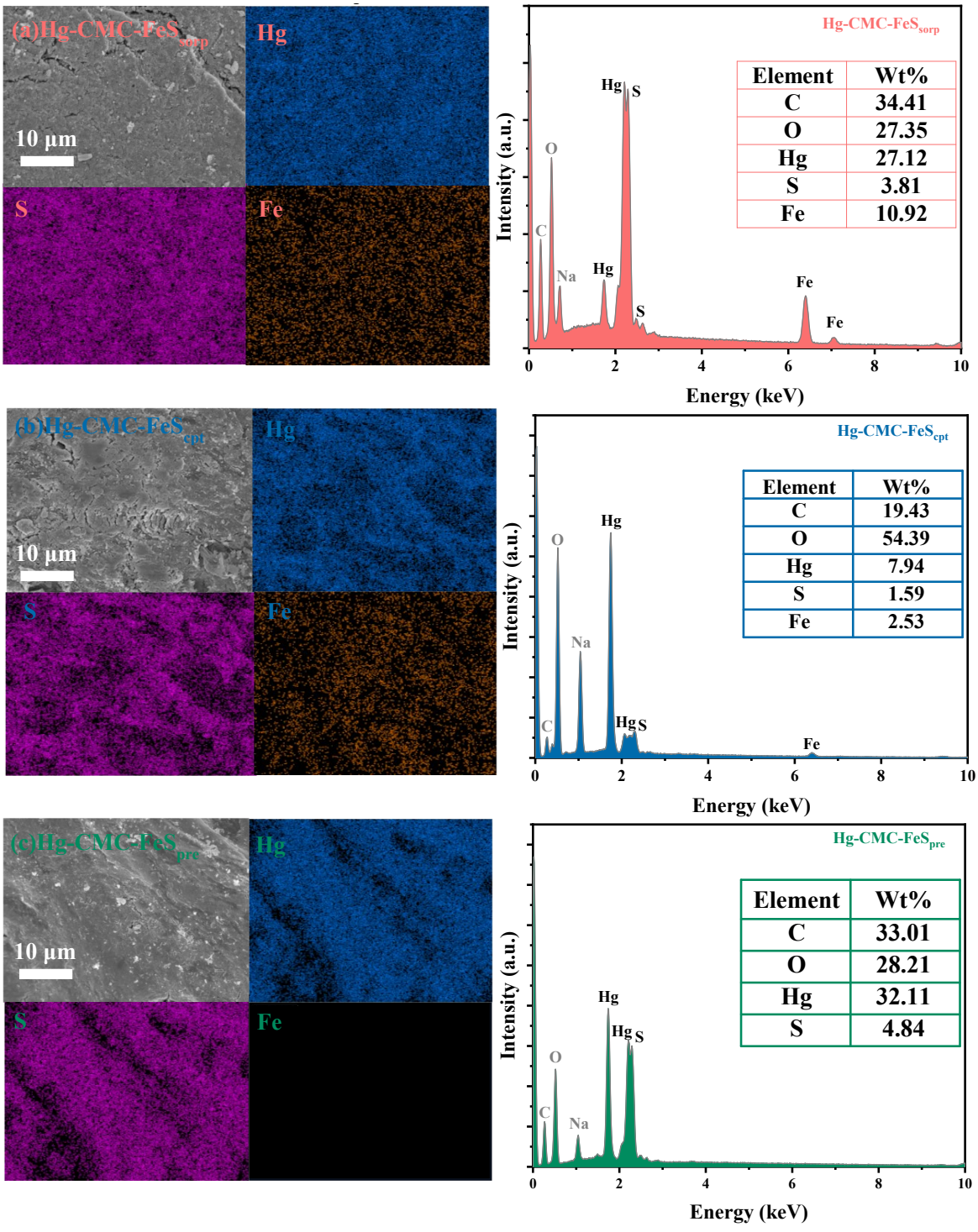

Figure S2. SEM-mapping and EDS of (a) Hg-CMC-FeS$_{sorp}$, (b) Hg-CMC-FeS$_{cpt}$, and (c) Hg-CMC-FeS$_{pre}$.

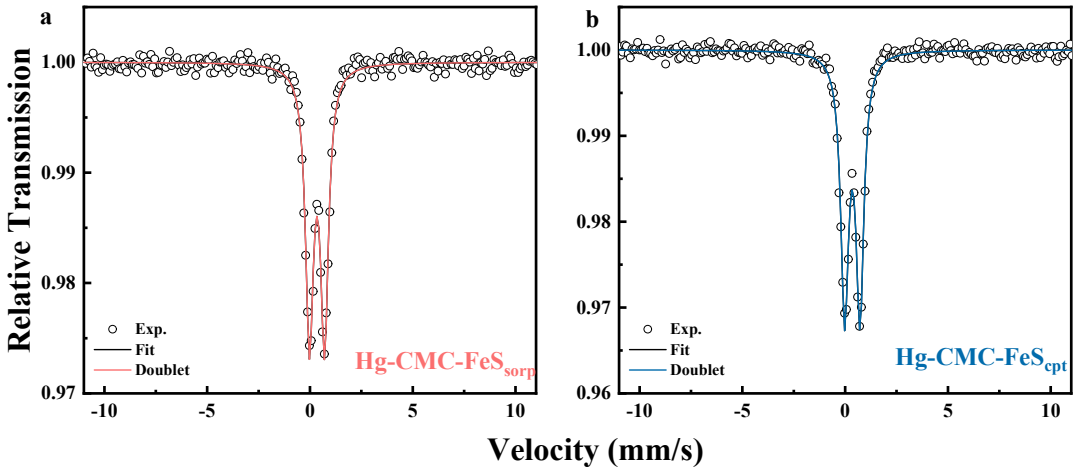

Figure S3. Mössbauer spectra of (a) Hg-CMC-FeS$_{sorp}$ and (b) Hg-CMC-FeS$_{cpt}$.

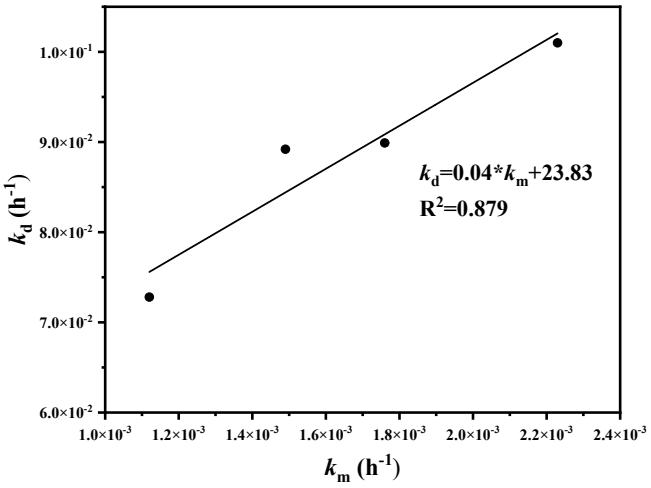

Figure S4. Linear relationship between methylation rate constant (k_m) and demethylation rate constant (k_d).

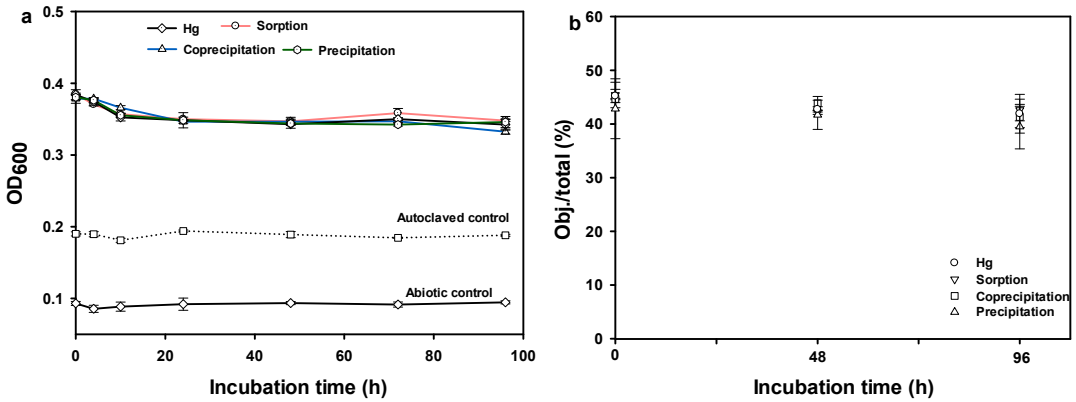

Figure S5. (a) Optical density (OD_{600}) and (b) activity of *G. sulfurreducens* PCA cultures exposed to Hg(II) after sorption, coprecipitation, and chemical precipitation with CMC-FeS. Hg(II) = 600 μg L^{-1}, CMC-FeS = 150 μg L^{-1}, pH = 7.0±0.2, and incubation time = 0-96 h. Data plotted as mean of duplicates and error bars (calculated as standard deviation) indicate data reproducibility.

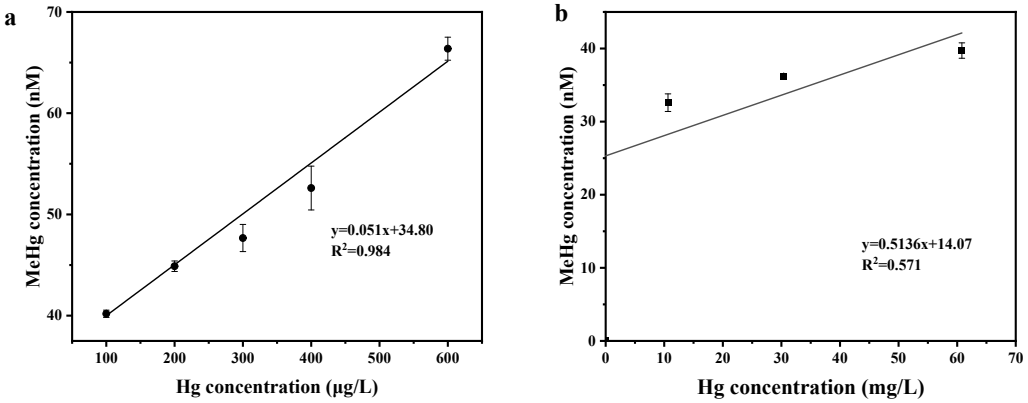

Figure S6. (a) MeHg production by *G. sulfurreducens* PCA cultures exposed to different concentrations of dissolved mercury and (b) MeHg production by *G. sulfurreducens* PCA cultures exposed to various concentrations of Hg in Hg-CMC-FeS_{cpt}. Data plotted as mean of duplicates and error bars (calculated as standard deviation) indicate data reproducibility.

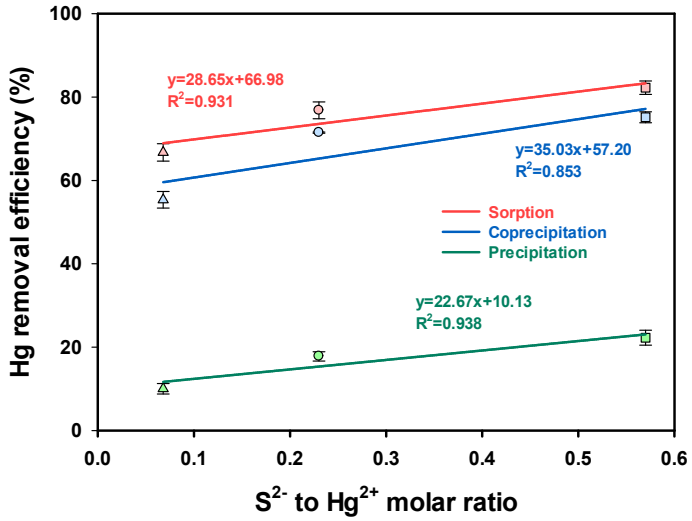

Figure S7. Linear relationship between S^{2-} to Hg^{2+} molar ratios and Hg(II) removal efficiency via sorption, coprecipitation, and precipitation with CMC-FeS. Hg(II) = 600 μg L^{-1}, S^{2-} to Hg^{2+} molar ratios = 0.068:1, 0.23:1 and 0.57:1, pH = 8.7±0.2, and reaction time = 48 h. Data plotted as mean of duplicates and error bars (calculated as standard deviation) indicate data reproducibility.

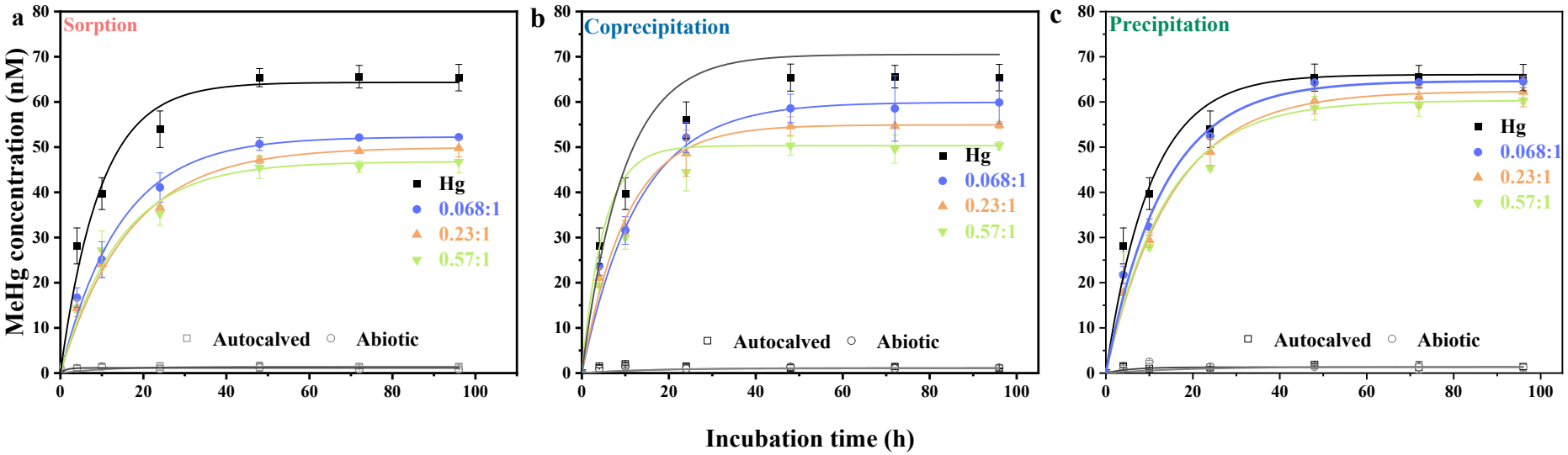

Figure S8. Dynamics of net mercury methylation by G. *sulfurreducens* PCA cultures exposed to Hg(II) before and after sorption, coprecipitation, and chemical precipitation with CMC-FeS at various S^{2-} to Hg^{2+} molar ratios. Hg = 600 μg L^{-1}, pH = 7.0±0.2, and incubation time = 0-96 h.

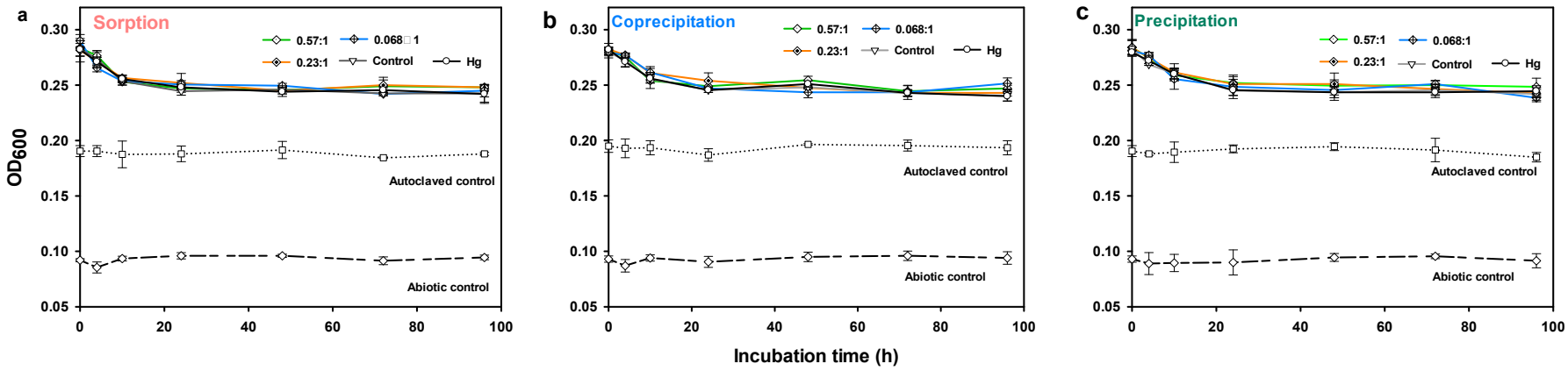

Figure S9. Optical density (OD_{600}) of *G. sulfurreducens* PCA cultures exposed to Hg(II) after (a) sorption, (b) coprecipitation, and (c) chemical precipitation with CMC-FeS. Hg= 600 µg L^{-1}, S^{2-} to Hg^{2+} molar ratios = 0.068, 0.23, and 0.57, pH = 7.0±0.2, and incubation time = 0-96 h. Data plotted as mean of duplicates and error bars (calculated as standard deviation) indicate data reproducibility.

1 Y. Gong, Y. Liu, Z. Xiong, D. Zhao, Immobilization of mercury by carboxymethyl cellulose stabilized iron sulfide nanoparticles: Reaction mechanisms and effects of stabilizer and water chemistry, *Environ. Sci. Technol.*, 2014, **48**, 3986-3994.

2 C. Liu, D. Guo, S. Wen, Y. Dang, D. Sun, P. Li, Transcriptomic insights unveil the crucial roles of cytochromes, NADH, and pili in Ag (I) reduction by *Geobacter sulfurreducens*, *Chemosphere*, 2024, **358**, 142174.

3 H. Muhamadali, Y. Xu, D. I. Ellis, J. W. Allwood, N. W. Rattray, E. Correa, H. Alrabiah, J.R. Lloyd, R. Goodacre, Metabolic profiling of *Geobacter sulfurreducens* during industrial bioprocess scale-up, *Applied and Environmental Microbiology,* 2015, **81**, 3288-3298.